2D SCRAMJET INLET DESIGN AND INVESTIGATION WITH COMPUTATIONAL FLUID DYNAMICS AND SUDDEN EXPANSION TUBE EXPERIMENTS

A THESIS SUBMITTED TO
THE GRADUATE SCHOOL OF NATURAL AND APPLIED SCIENCES
OF
MIDDLE EAST TECHNICAL UNIVERSITY

BY

YİĞİTCAN YANIK

IN PARTIAL FULFILLMENT OF THE REQUIREMENTS
FOR
THE DEGREE OF MASTER OF SCIENCE
IN
AEROSPACE ENGINEERING

APRIL 2023

Approval of the thesis:

2D SCRAMJET INLET DESIGN AND INVESTIGATION WITH COMPUTATIONAL FLUID DYNAMICS AND SUDDEN EXPANSION TUBE EXPERIMENTS

submitted by **YİĞİTCAN YANIK** in partial fulfillment of the requirements for the degree of **Master of Science** i**n Aerospace Engineering, Middle East Technical University** by,

Prof. Dr. Halil Kalıpçılar
Dean, Graduate School of **Natural and Applied Sciences** _____

Prof. Dr. Serkan Özgen
Head of the Department, **Aerospace Eng** _____

Prof. Dr. Sinan Eyi
Supervisor, **Aerospace Eng, METU** _____

Examining Committee Members:

Prof. Dr. Yusuf Özyörük
Aerospace Eng, METU _____

Prof. Dr. Sinan Eyi
Aerospace Eng, METU _____

Assoc. Prof. Dr. Nilay Sezer Uzol
Aerospace Eng, METU _____

Asst. Prof. Dr. Mustafa Perçin
Aerospace Eng, METU _____

Dr. Sıtkı Uslu
Mechanical Eng., TOBB ETU _____

Date: 17.04.2023

I hereby declare that all information in this document has been obtained and presented in accordance with academic rules and ethical conduct. I also declare that, as required by these rules and conduct, I have fully cited and referenced all material and results that are not original to this work.

Name Last name : Yiğitcan Yanık

Signature :

ABSTRACT

2D SCRAMJET INLET DESIGN AND INVESTIGATION WITH COMPUTATIONAL FLUID DYNAMICS AND SUDDEN EXPANSION TUBE EXPERIMENTS

Yanık, Yiğitcan
Master of Science, Aerospace Engineering
Supervisor: Prof. Dr. Sinan Eyi

April 2023, 47 pages

A 2D scramjet inlet is designed in this study specifically for operation at Mach 6 and 30 km altitude. The inlet design process is based on 1D performance estimations and included considerations for flow stability, shock wave patterns, and pressure recovery. The performance of the designed inlet is assessed using 2D and 3D CFD simulations and sudden expansion tube experiments at the TÜBİTAK SAGE facility.

It is found that the performance of the designed inlet is in good agreement with the 1D estimations at the design point, indicating that the inlet is feasible for operation under these conditions. Similar trends in pressure recovery and shock wave patterns are revealed by both the CFD simulations and sudden expansion tube experiments, with minor differences in the details of the flow field being observed.

This study provides insight into the design and performance of 2D scramjet inlets for operation at Mach 6 and 30 km altitude. Further work is needed to optimize the inlet design and study its performance under a wider range of conditions.

Keywords: Scramjet Inlet, Hypersonic Flow, Computational Fluid Dynamics, Sudden Expansion Tube

ÖZ

2 BOYUTLU SCRAMJET HAVA ALIĞI TASARIMI VE HESAPLAMALI AKIŞKANLAR DİNAMİĞİ VE ANİ GENİŞLEME TÜPÜ TESTLERİ İLE İNCELENMESİ

Yanık, Yiğitcan
Yüksek Lisans, Havacılık ve Uzay Mühendisliği
Tez Yöneticisi: Prof. Dr. Sinan Eyi

Nisan 2023, 47 sayfa

Bu çalışma kapsamında Mach 6 ve 30 km irtifa tasarım noktasına sahip bir 2D scramjet hava alığı tasarlanmıştır. Hava alığı tasarımı, 1 Boyutlu performans hesaplamaları ve akış kararlılığı, şok yapıları ve basınç toparlaması parametreleri gözetilerek gerçekleştirilmiştir. Tasarlanan hava alığı, 2 boyutlu ve 3 boyutlu hesaplamalı akışkanlar dinamiği analizleri ve TÜBİTAK SAGE Ani Genişleme Tüpü altyapısında gerçekleştirilen testler ile incelenmiştir.

Tasarlanan hava alığının performansının, 1 Boyutlu performans hesaplamaları ile uyumlu olduğu ve bu koşullarda başlatılabileceği tespit edilmiştir. Hesaplamalı akışkanlar dinamiği analiz sonuçları ile ani genişleme tüpü testlerinin sonuçları karşılaştırıldığında; basınç toparlaması değerlerinin ve şok yapılarının benzer olduğu gözlemlenmiştir.

Bu çalışma, Mach 6 ve 30 km irtifa tasarım noktası için 2 Boyutlu bir scramjet hava alığının tasarımı ve performans inceleme yöntemlerini ve sonuçlarını içermektedir. Hava alığı tasarımını optimize etmek ve daha geniş bir çalışma aralığına sahip olmasını sağlamak için gelecekte çalışmalar gerçekleştirilmelidir.

Anahtar Kelimeler: Scramjet Hava Alığı, Hipersonik Akış, Hesaplamalı Akışkanlar Dinamiği, Ani Genleşme Tüpü

ACKNOWLEDGMENTS

I would like to express my sincere gratitude to the following people and organizations for their invaluable assistance and support in the research and writing of this thesis.

First and foremost, I would like to thank my advisor, Prof.Dr. Sinan Eyi, for his constant guidance and sharing his expertise in the field of hypersonics. His encouragement and motivation are instrumental in completing this work, and I am deeply grateful for his invaluable mentorship.

I would like to thank Dr. Esra Başaran for her extensive help with the CFD simulations and her motivational support throughout the process. Her expertise and patience are invaluable, and I could not have completed this thesis without her guidance.

I would also like to Ali Kılıçkaya for his valuable contributions in revising the technical drawings of the scramjet inlet geometry. His attention to detail and thoroughness are essential in ensuring the accuracy of the design.

I am grateful to Bora Yazıcı and Dr. Bülent Sümer for providing me with access to the sudden expansion tube facility at TÜBİTAK SAGE and for their invaluable assistance in conducting the experiments. I would also like to thank Semra Gümrük Tokgöz for her company and support during the sudden expansion tube tests.

I would like to extend my appreciation to Sevda Serdarlar and Ayşe Bay for their motivational support and encouragement throughout the process of researching and writing this thesis. Their encouragement and kind words are greatly appreciated and helped me to stay motivated and focused.

I am deeply grateful to all the individuals and organizations who have contributed to this project.

TABLE OF CONTENTS

LIST OF TABLES

TABLES

LIST OF FIGURES

FIGURES

LIST OF ABBREVIATIONS

ABBREVIATIONS

CFD: Computational Fluid Dynamics

2D: 2 Dimensional

ICR: Internal Capture Ratio

CR: Contraction Ratio

CAD: Computer-aided Design

LIST OF SYMBOLS

SYMBOLS

M: $Mach\ Number$

T: $Temperature$

γ: $Specific\ Heat\ Ratio$

P: $Pressure$

A: $Area$

$\beta_1, \beta_2, \beta_3, \theta_1, \theta_2, \theta_3, x_1, x_2, x, h_1, h_2, h_3\ are\ given\ with$ Figure 3.1

Subscripts

t: $Stagnation$

0: $Freestream$

1: $First\ Ramp\ Shock$

2: $Second\ Ramp\ Shock$

3: $Cowl\ Shock$

CHAPTER 1

INTRODUCTION

1.1 Motivation

The design of scramjet engines and their components, particularly the inlet, has been the subject of extensive research in the field of aerospace engineering due to the potential for these engines to significantly improve the performance of hypersonic vehicles.

The inlet is an essential component of the scramjet engine, as it serves to compress and slow the incoming air to match the combustor operating conditions. The design of the inlet plays a crucial role in the overall performance of the engine and has been the focus of numerous studies[1]–[3]. However, the design of scramjet inlets is a complex task due to the high Mach number and high-temperature flow conditions present in the inlet. The presence of shock waves and boundary layer separation can lead to significant losses in inlet performance. Therefore, there is a need for improved design methodologies and optimization techniques for the development of efficient scramjet inlets[2], [3].

The goal of this study is to design a 2D scramjet inlet and investigate its performance through computational fluid dynamics (CFD) simulations and sudden expansion tube experiments. The CFD simulations will provide detailed information about the flow characteristics within the inlet, including the pressure, temperature, and velocity distribution. The sudden expansion tube experiments will allow for the measurement of the inlet's performance under actual operating conditions, providing valuable validation for the CFD simulations.

By carefully designing the inlet geometry and studying its flow characteristics, it is hoped that this work will contribute to the advancement of scramjet technology and provide insight into the optimization of inlet design for hypersonic vehicles. The results of this study may also have applications in the design of other high-speed propulsion systems, such as ramjets and supersonic combustion ramjets.

1.2 Background

Scramjet engines are a type of air-breathing propulsion system that has been the subject of numerous studies in the field of aerospace engineering due to their potential to significantly improve the performance of hypersonic vehicles. These engines operate by compressing and slowing the incoming air to match the combustor operating conditions, enabling them to reach high Mach numbers.

The design of scramjet engines and their components, particularly the inlet, has been the focus of extensive research due to the challenges associated with maintaining high-performance flow conditions within the inlet and combustor at high speeds and high temperatures. The presence of shock waves and boundary layer separation can lead to significant losses in performance.

To optimize the design of scramjet inlets, various techniques have been employed, including the use of computational fluid dynamics (CFD) simulations and optimization algorithms such as evolutionary-based optimization[3]. Experiments utilizing shock tubes and expansion tubes have also been utilized to validate the results of CFD simulations and study the performance of scramjet inlets under actual operating conditions[4].

In this study, a 2D scramjet inlet will be designed and its performance investigated through the use of CFD simulations and sudden expansion tube experiments. The results of this study will contribute to the understanding of scramjet inlet design and may have implications for the optimization of other high-speed propulsion systems.

1.3 Objectives

The primary objective of this study is to design a 2D scramjet inlet and investigate its performance using computational fluid dynamics (CFD) simulations and sudden expansion tube experiments.

Specific objectives of this study include:

- Designing a 2D scramjet inlet.
- Conducting 2D CFD simulations to study the flow characteristics within the inlet and compare them with design expectations.
- Conducting 3D CFD simulations to observe side-wall effects and 3D effects.
- Conducting sudden expansion tube experiments to validate the results of the CFD simulations.
- Contribute to the advancement of scramjet technology and provide insight into the inlet design for hypersonic vehicles.

Overall, the goal of this study is to design an efficient and high-performing scramjet inlet and investigate it through the use of CFD simulations and experiments.

1.4 Outline

This thesis, there are 5 chapters. Chapter 1 describes the motivation, background, objectives, and outline of the thesis.

In Chapter 2, a literature review on; scramjet inlets, their design methodologies, computational fluid dynamics analysis of scramjet inlets, and experiments with scramjet inlets are presented.

In Chapter 3, design methodology, computational fluid dynamics analysis methodology, and experimental methodology are presented.

In Chapter 4, designed scramjet inlet geometry, performance estimation of the inlet, computational fluid dynamics analysis results, data and images obtained in experiments, and data comparison of these performance investigation methods are presented.

Lastly, in Chapter 5, concluding remarks and future recommendations are presented.

CHAPTER 2

LITERATURE REVIEW

Scramjet and similar air-breathing hypersonic propulsion systems are important research topics in both the military and space industries due to their high flight speeds and specific impulse capabilities. The most suitable air-breathing engine for hypersonic flight is the supersonic combustion ramjet (scramjet). In a ramjet, the air entering the combustion chamber is decelerated to subsonic speeds and then accelerated through the nozzle to generate thrust. As flight speeds increase beyond 5 Mach, decelerating the air to subsonic conditions leads to increased shock losses and extremely high flow in the combustion chamber. The increased shock losses directly affect the engine efficiency, while the high temperatures in the combustion chamber can cause material and structural issues and chemical decomposition in the flow within the nozzle, resulting in energy loss[5]. Scramjet systems, in which the airflow is transmitted to the combustion chamber at supersonic speeds, are used to prevent these losses. A typical scramjet consists of three sub-systems as given in Figure 2.1: the inlet, the combustion chamber, and the nozzle.

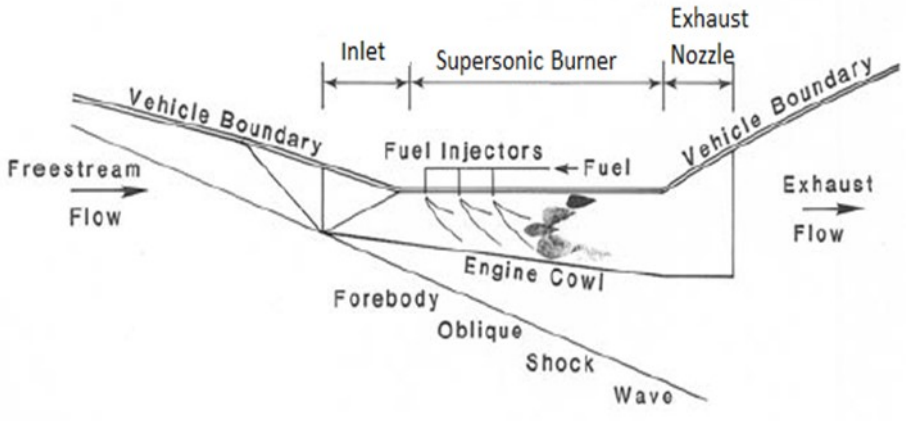

Figure 2.1. 2D Schematic of Scramjet Engine[6]

The role of the inlet in scramjet propulsion systems is to provide the desired static temperature ratio and static pressure ratio for a predetermined flight envelope, with maximum compression efficiency and total pressure recovery[6]. The air intake is a critical subsystem because it directly affects the starting phenomenon[6], total pressure recovery [7], and the flight envelope of the aircraft[3]. In the study, a scramjet air intake geometry is designed. The Matlab code is used to analyze geometry using computational fluid dynamics and sudden expansion tube experiments.

2.1 Historical Background

The key to the scramjet's operation is the ability to efficiently compress and heat the incoming air to allow for combustion to occur at supersonic speeds [5]. This is achieved through the use of a scramjet inlet, which is part of the engine responsible for the intake and compression of the incoming air[6]. There are several different types of scramjet inlets, including external compression, internal compression inlet, and mixed compression inlet[6]. The development of scramjet inlets has been a focus of research for many years and has involved both experimental and numerical methods, including wind tunnel testing [8], [9] and computational fluid dynamics (CFD) analysis [1]–[3].

Historical examples of scramjet development include the NASA Hyper-X program which aims to reach speeds of Mach 5 and served as a testbed for hypersonic technologies [10]and the HyShot scramjet flight experiment, which demonstrated the feasibility of scramjet propulsion[11]. More recent examples include the HIFiRE (Hypersonic International Flight Research Experimentation) program, which aims to advance the understanding of hypersonic flight and the development of scramjet technologies[12], and the X-51A Waverider, a hypersonic test vehicle that successfully demonstrated scramjet propulsion in a series of flights[13].

Despite significant progress in the development of scramjet inlets, challenges remain. One challenge is the ability to maintain stable and efficient operation at high speeds, as the high dynamic pressures and temperatures encountered in hypersonic flight can lead to instabilities and flow separation within the inlet Another challenge is the need to address the high temperatures and pressures encountered in hypersonic flight, which can lead to material and structural issues and require the use of specialized materials and cooling techniques[6].

Despite these challenges, the potential benefits of scramjet inlets, including their high specific impulse and the potential for efficient hypersonic flight, make them an important area of research and development. Future developments in scramjet inlet technology have the potential to revolutionize both military and civilian aviation and could enable the development of new hypersonic aircraft and space vehicles[6], [7].

2.2 Design of Scramjet Inlets

Several design and optimization methodologies are used for scramjet inlets in literature. Since the scope of this work is rectangular 2D scramjet inlets, 3 different design methodologies are investigated in this scope.

Kristen[14] designed a 2D scramjet inlet such that, ramp shocks intersect at the cowl lip at the design point and each oblique shock has equal strength. The designed inlet is a mixed compression inlet with 3 ramps and has Mach 4 design point. To find optimal inlet, total pressure ratio, adiabatic compression ratio, kinetic energy efficiency, and dimensionless entropy increase are investigated and optimized. Calculations of these parameters are made by “stream-thrust methodology”[6].

Brown[3], designed a 2D scramjet inlet such that, ramp shocks intersect at the cowl lip and the cowl shock intersect the shoulder, the internal capture ratio is less than 3, contraction ratio is less than 29. The designed inlet is an external compression inlet with 3 ramps and has Mach 10 design point. Combustor flow constraints are also used for the design of the inlet. Both sharp and blunted leading edge configurations

are investigated in this study. The maximum pressure recovery factor and minimum pressure recovery factor variance are aimed at by using the evolutionary-based algorithm. Designed geometry is investigated by computational fluid dynamics calculations. It is found that the average pressure recovery factor is less in the inviscid calculations than with a blunt leading edge and viscous properties.

Torrez[2], designed a 2D scramjet inlet such that, ramp shocks have equal strength, ramp shocks intersect at the cowl lip, the first cowl shock goes downstream of the shoulder and internal shocks reflect downstream of the shoulder. It operates in a design range of flight Mach number and angle of attack. The designed inlet is an external compression inlet with 5 ramps and has Mach 7 to 9 design range.

2.3 Computational Fluid Dynamics for Scramjet Inlets

Many studies investigate scramjet inlets with computational fluid dynamics calculations. 3 different works are reviewed in this part.

Idris[1], used CFD to investigate a 2D scramjet inlet, which has a design point Mach number of 5, on-design and off-design performance. SST k-w model turbulence model with Low-Reynolds number correction is used. ANSYS Fluent software is used as a solver. The Solver setup is density based and has second-order accuracy by Second Order Spatially Accurate Upwind Scheme. Roe's Flux-Difference Splitting is chosen in this study. Boundary conditions are taken from experimental conditions. Quadrilateral cells are used in the mesh. Wall and flow pressures are investigated in this study to compare with the measurements taken from the experiments. Numerical Schlieren images are also generated to compare with the experimental Schlieren images.

Nguyen[8], used CFD to investigate the sidewall compression effect and relaminarization phenomenon in a 3D scramjet inlet. A research code, QUADFLOW[15] is used as a solver. The Solver setup has second-order accuracy. The flux splitting scheme is taken from the work of Wada and Liou [16]. An explicit

5th-order Runge-Kutta scheme is used for calculations. The turbulence model is the k-w model. Flow structures, pressure, and temperature distributions are investigated to see the sidewall effect and results are compared with experimental measurements.

Su[17], used CFD to investigate the transient accelerative restarting process of a 3D scramjet inlet. SST k-w turbulence model is used with compressibility corrections[18]. Monotone Upstream-Centered Schemed for Conservation Laws (MUSCL) scheme is preferred to increase accuracy. Restarting phenomenon is investigated for a flight trajectory by using wall pressure and flow pressure and Mach number distributions.

2.4 Experimental Work on Scramjet Inlets

Idris[1], made experimental work in the University of Manchester's High Supersonic Tunnel Facility (HSST) which is a blowdown supersonic tunnel. 2 ramp scramjet inlet model is used in experiments at Mach 5. A Z-type color-schlieren setup is used in experiments. To obtain wall static pressure distribution, 18 pressure tappings, and 6 transducers are used in ramps, therefore, each test requires three runs and to do a repeatability analysis each test requires two runs which results in a 6 test for the test each case. Pressure-sensitive paint is also applied to investigate inlet pressure distribution at the external flow field. The infrared thermal imaging technique is also used in the experiments to obtain temperature distribution. Experiment results are compared with design calculations and CFD analysis results to verify the design model.

Hohn[19], made experimental work in a hypersonic blowdown wind tunnel. Single ramp scramjet inlet is used in experiments at Mach 7. 55 pressure tappings are used in the inlet model such that 30 tappings at the lower wall center line, 13 tappings at the upper wall and cowl, 12 pressure tappings in two circumferential cross-sections. A cross-shaped pitot rake is used to measure total and static pressure distribution. Infrared thermography is used to evaluate heat fluxes on the ramp. Experimental

results are used to investigate the effect of variable internal contraction in a 3D scramjet inlet.

Haberle[20], made experimental work in a hypersonic wind tunnel (H2K). 2 ramp scramjet inlet is used in experiments on Mach 7. The shadowgraph technique is used to visualize the flow. To measure the captured flow rate a rotational symmetric flow meter is used with a conical plug to simulate combustion chamber pressure. Infrared thermography is used to obtain surface temperatures and evaluate wall heat fluxes. Experiment results are used to investigate the 2D scramjet inlet flow field.

CHAPTER 3

METHODOLOGY

In this section, the scramjet inlet design method, performance estimation method, and design verification method are given. In the examination of the designed scramjet inlet, Matlab code prepared for performance estimation computational fluid dynamics analyses and sudden expansion tube experiments is used. Oblique shock relations are used in the related performance estimation calculations. Similar studies in the literature are used to verify the computational fluid dynamics analysis method.

3.1 Scramjet Inlet Design and Performance Estimation

In this section, the scramjet inlet design point, design method, design limits, and performance estimation method are given. While determining the dimensional limits of the air intake designed for scramjet inlet studies, the dimensions of the TÜBİTAK SAGE Sudden Expansion Tube test chamber and imaging area are considered. Considering the dimensional limits and design options, it is decided to use an air intake with 2 ramps. An altitude of 30 kilometers and a flight condition of Mach 6 are chosen as the inlet design point.

The geometric parameters used while designing the scramjet inlet are given in Figure 3.1.

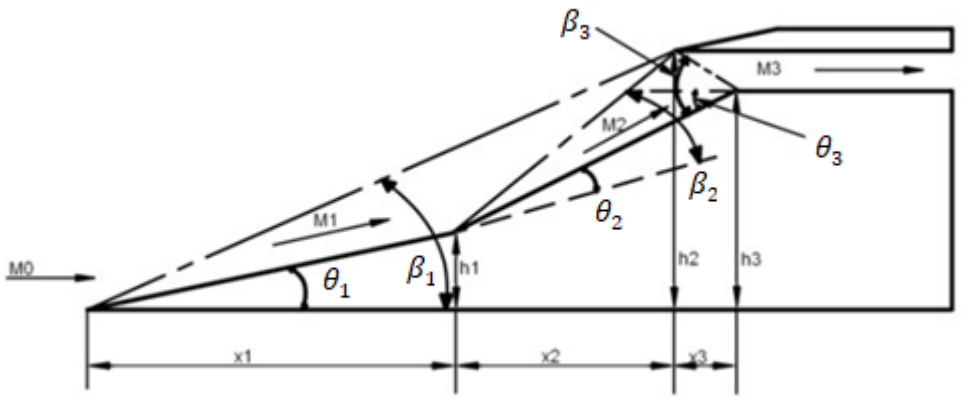

Figure 3.1. Scramjet Inlet Geometric Parameters[1]

When starting the scramjet inlet design, ramp oblique shocks must be taken into account first. Relevant calculations have been made to ensure that the ramp shocks intersect at the cowl lip. To reach maximum performance, the pressure ratios of the ramp oblique shocks should be equal[5]. The equations used for the relevant calculations are given with equations 3.1-3.9 The limits used while performing the scramjet inlet design are given in the Design Limits section. The geometric design results are obtained with iterative solutions performed with the Matlab code prepared by using the given limits and equations.

$$M_1 = \frac{1}{\sin(\beta_1 - \theta_1)} \sqrt{\frac{1 + \frac{\gamma - 1}{2} * M_0^2 * \sin^2 \beta_1}{\gamma * M_0^2 * \sin^2 \beta_1 - \frac{\gamma - 1}{2}}} \quad 3.1$$

$$M_2 = \frac{1}{\sin(\beta_2 - \theta_2)} \sqrt{\frac{1 + \frac{\gamma - 1}{2} * M_1^2 * \sin^2 \beta_2}{\gamma * M_1^2 * \sin^2 \beta_2 - \frac{\gamma - 1}{2}}} \quad 3.2$$

$$M_3 = \frac{1}{\sin(\beta_3 - \theta_3)} \sqrt{\frac{1 + \frac{\gamma - 1}{2} * M_2^2 * \sin^2 \beta_2}{\gamma * M_3^2 * \sin^2 \beta_3 - \frac{\gamma - 1}{2}}} \quad 3.3$$

$$\theta_3 = \theta_1 + \theta_2 \quad 3.4$$

$$\frac{h_1}{x_1} = \tan(\theta_1) \quad 3.5$$

$$\frac{h_2}{x_1 + x_2} = \tan(\beta_1) \quad 3.6$$

$$\frac{h_2 - h_1}{x_2} = \tan(\beta_2 + \theta_1) \quad 3.7$$

$$\frac{P_{t_1}}{P_{t_0}} = \left(\frac{(\gamma+1) * M_0^2 * \sin^2\beta_1}{(\gamma-1) * M_0^2 * \sin^2\beta_1 + 2}\right)^{\frac{\gamma}{\gamma-1}} * \left(\frac{\gamma+1}{2*\gamma*M_0^2*\sin^2\beta_1 - (\gamma-1)}\right)^{\frac{1}{\gamma-1}} \quad 3.8$$

$$\frac{P_{t_2}}{P_{t_1}} = \frac{P_{t_1}}{P_{t_0}} \quad 3.9$$

Oblique shock relations are used while performing the air intake performance estimation, as given with equations 3.10-3.13.

$$\frac{T_{i+1}}{T_i} = \frac{(2*\gamma*M_i^2*\sin^2\beta_{i+1} - (\gamma-1)) * (\gamma-1) * M_i^2 * \sin^2\beta_{i+1} + 2}{(\gamma+1) * M_i^2 * \sin^2\beta_{i+1}} \quad 3.10$$

$$\frac{P_{i+1}}{P_i} = \frac{(2*\gamma*M_i^2*\sin^2\beta_{i+1} - (\gamma-1))}{(\gamma+1) * M_i^2 * \sin^2\beta_{i+1}} \quad 3.11$$

$$M_{i+1} = \frac{1}{\sin(\beta_{i+1} - \theta_{i+1})} \sqrt{\frac{1 + \frac{\gamma-1}{2} * M_i^2 * \sin^2\beta_{i+1}}{\gamma * M_i^2 * \sin^2\beta_{i+1} - \frac{\gamma-1}{2}}} \quad 3.12$$

$$\frac{P_{t_{i+1}}}{P_{t_i}} = \left(\frac{(\gamma+1) * M_i^2 * \sin^2\beta_{i+1}}{(\gamma-1) * M_i^2 * \sin^2\beta_{i+1} + 2}\right)^{\frac{\gamma}{\gamma-1}} * \left(\frac{\gamma+1}{2*\gamma*M_i^2*\sin^2\beta_{i+1} - (\gamma-1)}\right)^{\frac{1}{\gamma-1}} \quad 3.13$$

3.1.1 Design Limits

Scramjet inlet design limits are given in this section.

- The total length of the scramjet inlet must not be longer than 220mm to be tested in the TÜBİTAK SAGE Sudden Expansion Tube.
- The ratio of the inlet's outlet Mach number and freestream Mach number (M0) must be above 0.38[6].

Kantrowitz limit, internal contraction ratio, and contraction ratio are used for the inlet starting limit. The internal capture is the ratio of the inlet cowl area to the inlet throat area. When this ratio is above 3, the inlet will not start[7]. The contraction ratio is the ratio of the total capture area to the inlet throat area. The contraction ratio maximum limit is a function of the Mach number. If the relevant limit is exceeded, a started air intake may return to a non-starting state[7]. Related equations are given with Equations 14, 15, and 16 respectively.

$$\left(\frac{A_e}{A_i}\right)_k = \left(\frac{\gamma-1}{\gamma+1}+\frac{2}{(\gamma+1)*M_2^2}\right)^{0.5} * \left(\frac{2*\gamma}{\gamma+1}-\frac{\gamma-1}{(\gamma+1)*M_2^2}\right)^{\frac{1}{\gamma-1}} * \frac{\sin(\beta_1-\theta_1)}{\sin(\beta_1)} * \frac{\sin(\beta_2-\theta_2)}{\sin(\theta_1)} \quad 3.14$$

$$where \frac{A_e}{A_i} = \frac{h_2-h_3}{h_2}$$

$$CR = \frac{h_2 - \frac{x_3}{\tan(\theta_3)}}{h_2-h_3} \leq 3 \quad 3.15$$

$$CR = \frac{h_2}{h_2-h_3} \quad 3.16 \text{ and } CR_{max} = \left(0.05 - \frac{0.52}{M_0} + \frac{3.65}{M_0^2}\right)^{-1} \quad 3.17$$

- While determining the combustion chamber inlet limits, hence the inlet's outlet limits; static temperature, static pressure, and Mach number limits are used. The static temperature range suitable for spontaneous and rapid combustion in the combustion chamber is between 1100K and 1700K, and the static pressure range is between 50kPa and 1 MPa[21]. If it is high, very

high lengths of combustion chambers are needed to provide the necessary time for the combustion reactions to take place in the combustion chamber. The fact that the combustion chamber inlet Mach number is between 2.2 and 5 prevents these problems[22].

3.2 Investigation of Scramjet Inlet with Computational Fluid Dynamics

In this section, the CFD analysis model to be used within the scope of scramjet inlet design investigation studies is given. CFD analysis is used as the scramjet inlet design verification method. Studies started with the verification of the numerical method. While validating the numerical method, a scramjet inlet geometry with 2 ramps is used, which has already been validated by CFD analysis and experiments. After the numerical model is established, the boundary conditions are determined, and the mesh is created. The mesh dependency study is also carried out. The geometry used when performing the numerical method validation is given in Figure 3.2.

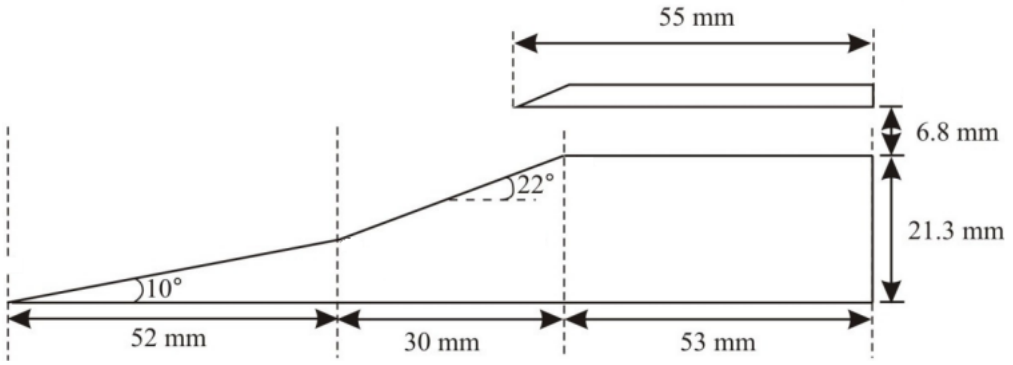

Figure 3.2. 2D Scramjet Inlet Geometry Used In Numerical Verification Study[1]

The numerical model used within the scope of validation and analysis studies is given in Table 3.1. Boundary conditions are taken as flight speed 5 Mach, static temperature 62.5 K, and static pressure 1220 Pa[1]. Within the scope of mesh dependency studies, 3 different meshes are established. While the related solution meshes are being installed, it is ensured that the y+ values at the walls are below 1. The maximum element widths of 1mm, 0.5mm, and 0.25mm, and the cell numbers are obtained as 41576, 83012, and 166024, respectively. Related meshes are given in Figure 3.3, Figure 3.4, and Figure 3.5, respectively.

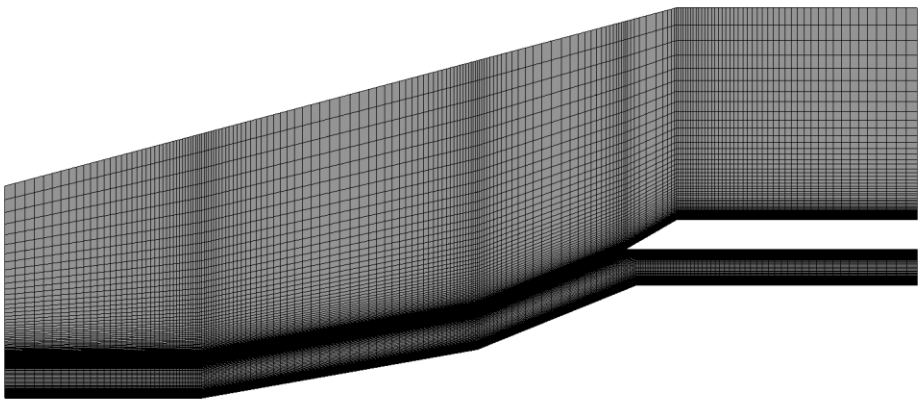

Figure 3.3. Mesh Dependency Study Mesh # 1 – Verification Case

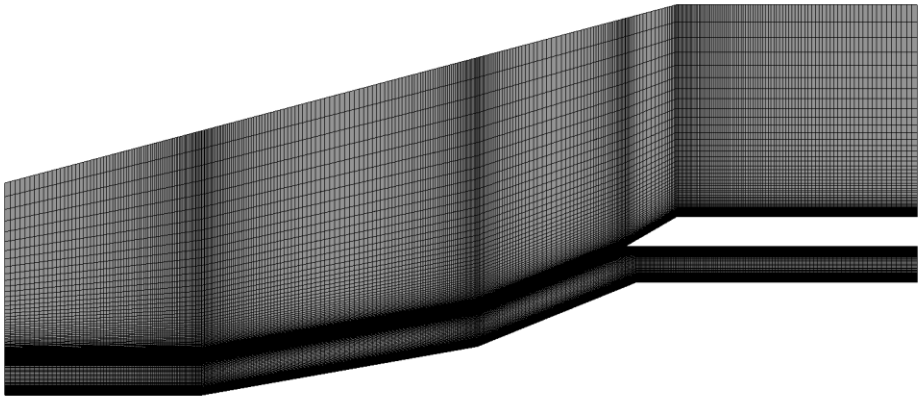

Figure 3.4. Mesh Dependency Study Mesh # 2 – Verification Case

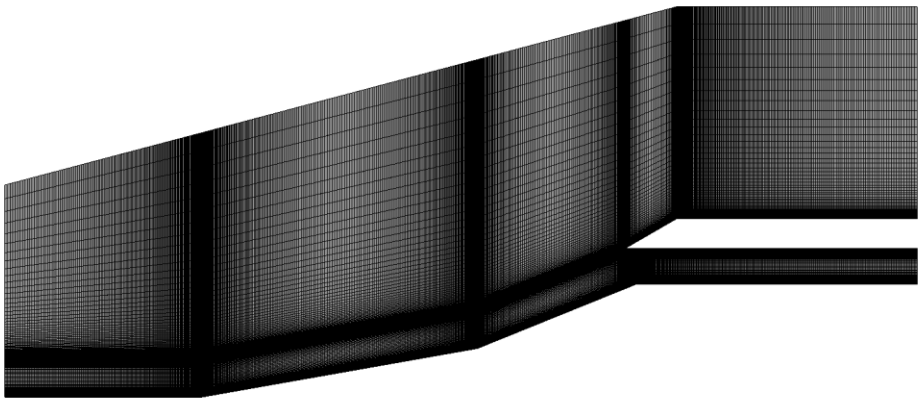

Figure 3.5. Mesh Dependency Study Mesh # 3 – Verification Case

The final mesh properties obtained as a result of mesh dependency studies are used to create the mesh of the designed inlet geometry. In the inlet design method verification, first, inviscid CFD analysis is performed because the design is designed with a non-viscous flow assumption. After the related study, the performance of the designed inlet geometry under viscous effects and boundary layer interactions on the

geometry is investigated. The numerical method, mesh, and CFD analysis results used in this study are given in the Investigation of Scramjet Inlet with 2D Computational Fluid Dynamics section.

Table 3.1 Solver Settings

Solution Model	. Density Based
Turbulence Model	SST k-omega
Spatial Discretization	Second Order Upwind
Wall y+ Values	y+ < 1

The properties of the meshes obtained within the scope of mesh dependency studies and the parameters controlled in the dependency studies are given in

Table 3.2. The numerical Schlieren image obtained from CFD analysis performed with Mesh # 2 and the image obtained from the test performed in the literature are given in Figure 3.6 and Figure 3.7 respectively. When the sensitivity ratio parameters are examined, it is concluded that Mesh # 2 for numerical model validation studies is appropriate to use, since the sensitivity rates between Mesh # 3 and Mesh # 2 are below 1% and the outlet velocity distribution is similar. After the numerical model is verified, the scramjet inlet geometry CFD analyses are carried out with the solution mesh to be created using similar cell sizes with Solution Mesh 3 to increase the numerical Schlieren image resolution. The related mesh option and CFD analyses are given in the Investigation of Scramjet Inlet with 2D Computational Fluid Dynamics section. For all CFD analyses performed within the scope of the study; it has been ensured that all residual values fall below the level of 10-4, the average Mach number at the isolator outlet, the static pressure, the total pressure, and the mass flow rate are fixed, and the total mass flow rate in the control volume reaches 0.

Table 3.2 Mesh Dependency Study

Mesh #	Maximum Cell Size[mm]	Mesh Element Count[#]	Outlet Average Static Pressure[Pa]	Outlet Average Mach Number[#]	Outlet Average Mass Flow Rate [kg/s]	Relative Difference (Respectively)[%]
1	1	41576	23012	1.98	1.432	-
2	0.5	83012	23372	1.96	1.42	1.56 - 1.01 - 0.83
3	0.25	166024	23577	1.94	1.425	0.87 -1.02 - 0.35

Figure 3.6. Numerical Schlieren - Verification Case

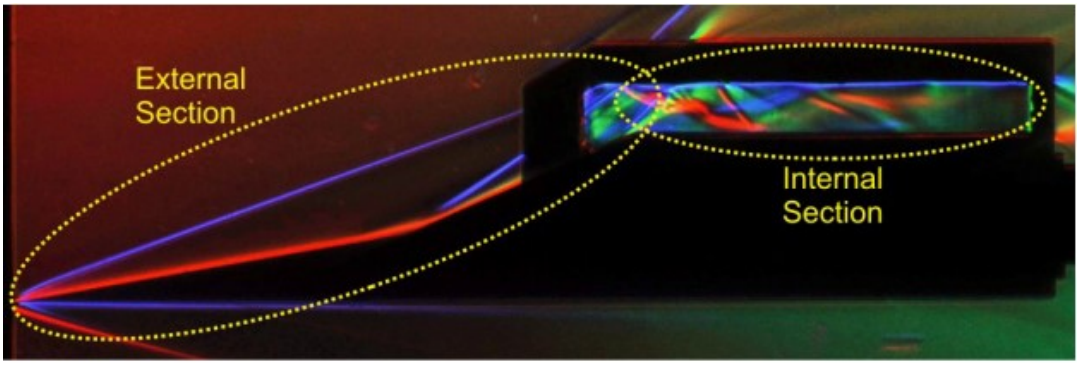

Figure 3.7. Color Experimental Schlieren [1]

In the verification process of the numerical model, pressure measurements and Schlieren images in the tests performed with the scramjet inlet geometry given in Figure 3.2 are used. All pressure measurements are taken on the ramp[1], and the comparison with the CFD analysis results for different mesh options are given in

Figure 3.8. When the results are examined, it is observed that the CFD analysis results are quite close to the test results. When the Schlieren images given in Figure 3.6 and Figure 3.7 are examined, it is observed that the ramp shock structure is similar, and the shock and separation phenomena in the isolator occur at similar points. In the scope of numerical model validation and mesh dependency studies, it is decided to use the described numerical model and mesh methodology for CFD analysis of the designed scramjet inlet.

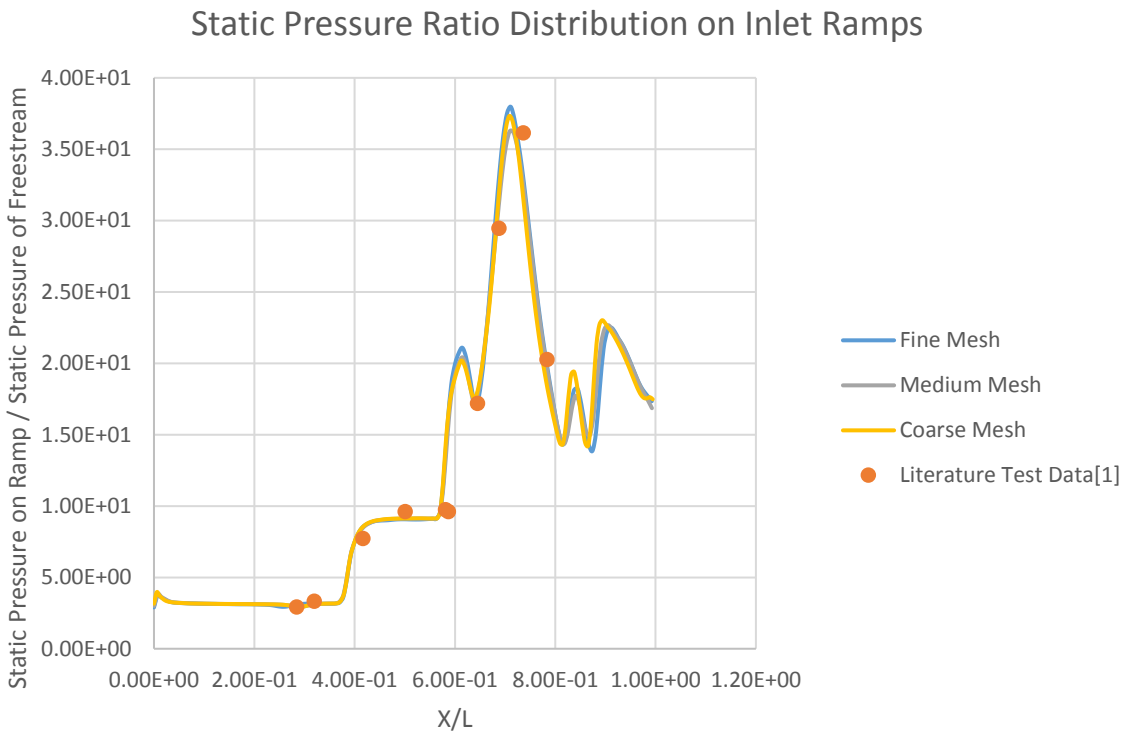

Figure 3.8. Comparison of Static Pressure Ratio Distribution on Inlet Ramps

3.3 Investigation of Scramjet Inlet with Sudden Expansion Tube Experiments

Experiments focusing on scramjet inlets are conducted utilizing the TUBITAK SAGE Sudden Expansion Tube, an impulse flow test system designed to produce

short-duration, high-speed flow conditions. This facility played a crucial role in the investigation of scramjet inlet performance under various circumstances.

Before initiating the scramjet inlet experiments within the sudden expansion tube, a series of calibration tests are performed to ensure accurate and reliable results. A double wedge with a 20° half-wedge angle is employed for these calibration tests, as illustrated in Figure 3.9. Schlieren images captured during the tests served as a valuable tool for determining the appropriate filling pressures for achieving Mach 6 conditions. The outcomes of these calibration tests are presented in

Table 3.3, while a Schlieren image from Test 2 can be observed in Figure 3.10.

To maintain consistency and minimize potential discrepancies, all calibration tests are conducted under identical conditions. Based on the established error margins, it is determined that the subsequent inlet experiments should also be carried out under the same controlled conditions for optimal results.

Figure 3.9. Double Wedge - Calibration Tests

Table 3.3. Calibration Test Results

	Test1	**Test2**	**Test3**
Shock Angle[°]	28.5±0.5	28.25±0.4	28.4±0.5
Mach Number[#]	5.8±0.4	6.0±0.3	5.9±0.4

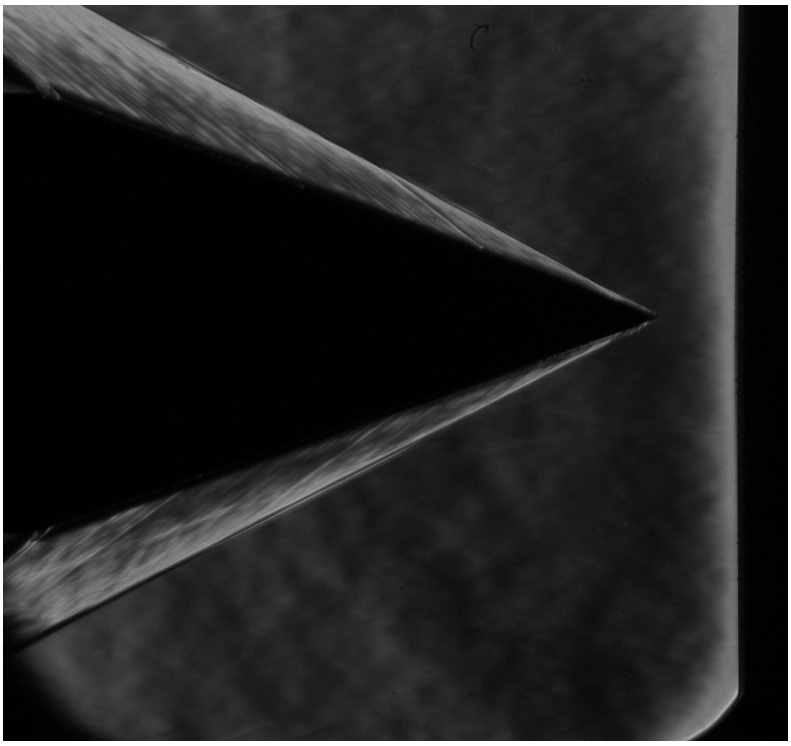

Figure 3.10. Schlieren Image - Calibration Test2

The scramjet inlet experiments are conducted under specific test room conditions, including a Mach 6 flow velocity, a static pressure of 41.6 kPa, and a static temperature of 243.3 K. Schlieren imaging techniques are employed to capture and analyze the oblique shock angles generated within the flow field.

The acquired Schlieren images will be compared with numerical Schlieren images to ensure the validity of the experimental results. Furthermore, the oblique shock angles measured from these images will be utilized to compute flow properties within the scramjet inlet flow field. These calculated values will then be compared with one-dimensional analysis and computational fluid dynamics (CFD) results to evaluate their consistency and accuracy.

A computer-aided design (CAD) model of the scramjet inlet utilized in these experiments is shown in Figure 3.11, while the actual manufactured test article for the scramjet inlet is given in Figure 3.12.

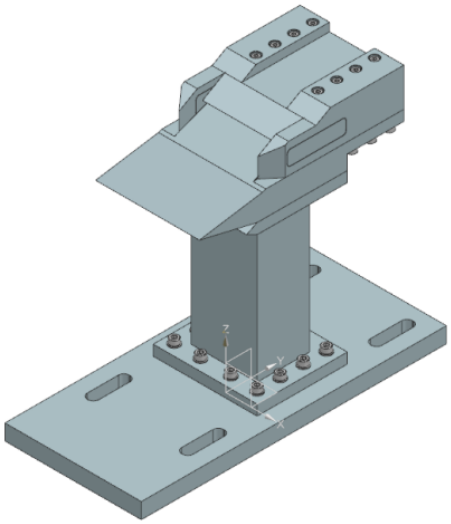

Figure 3.11. CAD Model of Scramjet Inlet Test Article

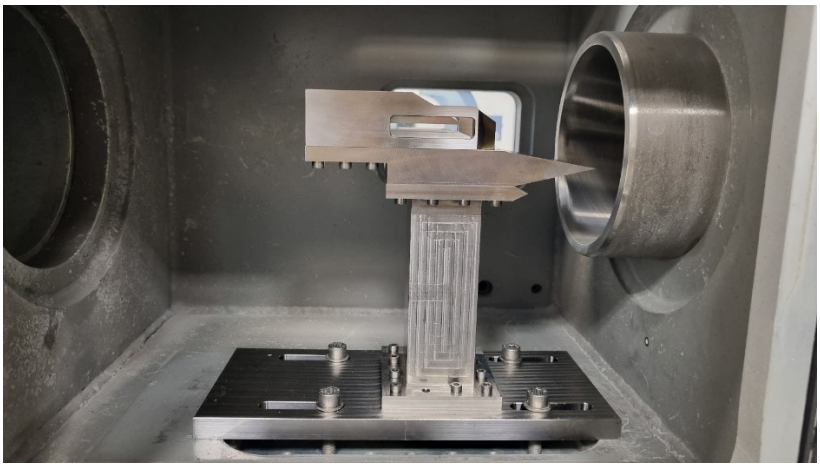

Figure 3.12. Scramjet Inlet Test Article in Sudden Expansion Tube Test Section

CHAPTER 4

RESULTS AND DISCUSSION

Designed scramjet inlet geometry, predicted performance with 1D calculations, investigated the inlet with CFD, and sudden expansion tube experiments and comparison of the results are presented in this section.

4.1 Scramjet Inlet Design Calculations and Predicted Performance

The designed 2D scramjet inlet geometry dimensions are given in Figure 4.1. Predicted performance parameters that are calculated at the design point are given in Table 4.1.

.

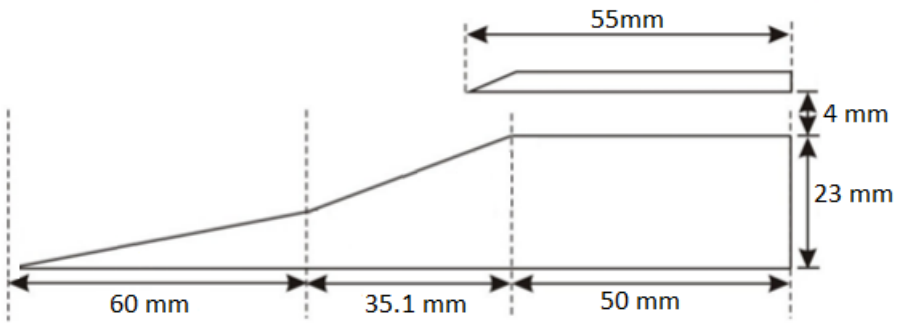

Figure 4.1. Designed 2D Scramjet Inlet

Table 4.1 Predicted Performance Parameters of the Designed Inlet

Parameter	Value	Parameter	Value
M_1	4.73	P_{s1}	3.980 kPa
M_2	3.64	P_{s2}	13.610 kPa
M_3	2.30	P_{s3}	68.280 kPa
T_1	346.90 K	P_{t1}	15.267 bar
T_2	519.50 K	P_{t2}	12.714 bar
T_3	923.20 K	P_{t3}	8.525 bar

4.2 Investigation of Scramjet Inlet with 2D Computational Fluid Dynamics

In the scope of design investigation studies, 3 different CFD analysis cases are carried out after the mesh dependency study. The properties of the meshes obtained within the scope of mesh dependency studies and the parameters controlled in the dependency studies are given in Table 4.2. When the sensitivity ratio parameters are examined, it is concluded that Mesh # 2 for numerical model validation studies is appropriate to use, since the sensitivity rates between Mesh # 3 and Mesh # 2 are below 1% and the outlet velocity distribution is similar.

Table 4.2 Mesh Dependency Study – Designed Inlet – Viscous Case

Mesh #	Maximum Cell Size[mm]	Mesh Element Count[#]	Outlet Average Static Pressure[Pa]	Outlet Average Mach Number[#]	Outlet Average Mass Flow Rate [kg/s]	Relative Difference (Respectively)[%]
1	1	55788	45900	2.26	0.690	-
2	0.5	112160	42750	2.33	0.700	6.9 – 3.1 – 1.5
3	0.25	151360	42400	2.35	0.705	0.8 -0.9 - 0.7

First, an inviscid CFD analysis model is created, since the related scramjet inlet is designed with an inviscid flow assumption. The mesh used in the relevant model is given in Figure 10. The related mesh has a maximum cell size of 0.5mm and consists of a total of 112160 cells. Freestream information is used for boundary conditions, Mach 6 flight speed, 1161.18 Pa static pressure, and 231.61 static temperature values, which are the flight conditions for 30km altitude, are used. Wall temperatures are assumed to be constant. The numerical Schlieren image obtained as a result of the related CFD analysis is given in Figure 4.2. In the related image, it can be seen that the ramp shocks are at the cowl lip as expected. Investigation studies are also carried out with a comparison of the related inviscid CFD analysis, and the 1D performance estimation results are given in Table 4.3. The related results are mass-weighted averages. It is assumed that the deviations are within an acceptable range.

Figure 4.2. Numerical Schlieren – Inviscid Case

Table 4.3 Comparison of Inviscid CFD Analysis and 1D Performance Estimation

Parameter	**Value**	**Relative Difference(%)**	**Parameter**	**Value**	**Relative Difference(%)**
M_1	4.74	0.21	P_{s1}	3.920	1.53
M_2	3.65	-0.27	P_{s2}	13.626	0.12
M_3	2.41	4.56	P_{s3}	66.690	2.38
T_1	343.00	1.14	P_{t1}	18.420	17.12
T_2	518.00	0.29	P_{t2}	15.060	15.58
T_3	887.00	4.08	P_{t3}	10.300	17.23

After the completion of the validation work, CFD analysis is performed to examine the viscous effects and the performance of the scramjet inlet in viscous media. The mesh used in the related CFD analysis is given in Figure 4.3. The maximum cell size of the related mesh is 0.5mm and consists of a total of 112160 cells. The numerical model used in the related CFD analysis is given in Table 3.1. Freestream information is used for boundary conditions, Mach 6 flight speed, 1161.18 Pa static pressure, and 231.61 static temperature values are used. The numerical Schlieren image obtained from the CFD analysis is given in Figure 4.4. When the given Schlieren image is examined, the deviation in the ramp shocks and the flow separation at the end of the ramp is observed. The inlet performance in viscous media and its deviation from the inviscid flow assumption is given in Table 4.4. Ignoring viscous effects while designing the air intake geometry leads to a change in viscous media performance due to boundary layer and shock interactions[1]. Relevant performance changes are also seen in the given Schlieren image and performance parameters.

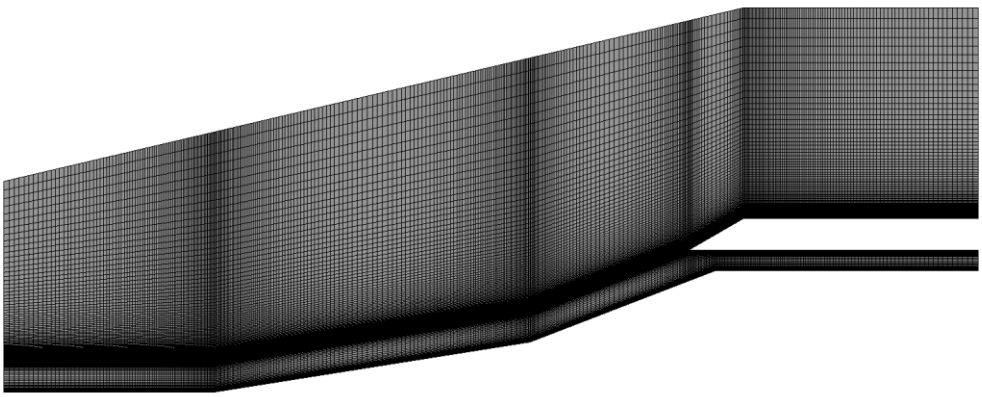

Figure 4.3. Mesh # 2 for Designed Inlet Case

Figure 4.4. Numerical Schlieren – Designed Inlet Case – Viscous Solution

Table 4.4 Comparison of Viscous CFD Analysis and Inviscid CFD Analysis

Parameter	**Value**	**Relative Difference(%)**	**Parameter**	**Value**	**Relative Difference(%)**
M_1	4.62	2.60	P_{s1}	4.39 kPa	-10.71
M_2	3.54	3.11	P_{s1}	14.05 kPa	-3.02
M_3	2.16	11.57	P_{s3}	74.12 kPa	-10.02
T_1	355 K	-3.38	P_{t1}	17.3 bar	6.47
T_2	540 K	-4.07	P_{t1}	13.2 bar	14.09
T_3	980 K	-9.49	P_{t3}	8.9 bar	15.73

The obtained contours, numerical Schlieren image, performance parameters, and the performance of the inlet in viscous media are investigated. It has been determined that the designed inlet can be started in a viscous environment and at the related design point and performs close to the expected performance. Lastly, a viscous CFD analysis is done for sudden expansion shock tube test room conditions with the same mesh and solver settings. Mach 6 flight speed, 41.642 kPa static pressure, and 243.3 K static temperature are used for boundary conditions. The results of this analysis will be compared with sudden expansion tube experiments in Section 4.3. Investigation of Scramjet Inlet with 3D Computational Fluid Dynamics.

A three-dimensional (3D) computational fluid dynamics (CFD) analysis is conducted to study the presence and influence of 3D flow structures on scramjet inlet performance and side-wall interactions. The inlet geometry used for the analysis is displayed in Figure 4.5. Mesh and solver settings are provided in Table 4.5.

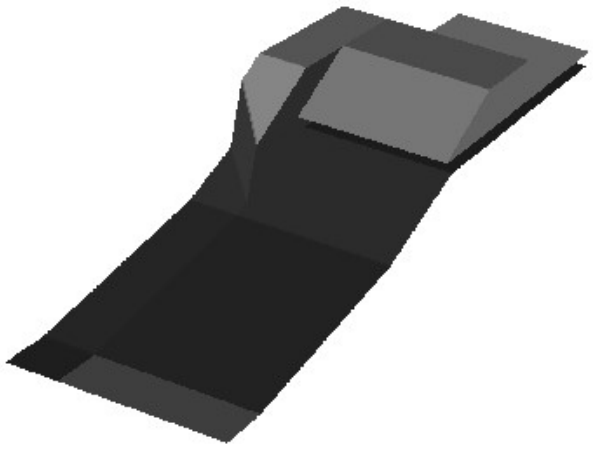

Figure 4.5 Inlet Geometry Used in 3D CFD Analysis

Table 4.5 Mesh and Solver Settings

Mesh Type	Hexcore
Cell Count	17081455
Max Cell Width	0.5 mm
Solution Model	Density Based
Turbulence Model	SST k-omega
Spatial Discretization	First Order Upwind
Wall y+ Values	y+<1

A comparative analysis is conducted using the Sudden Expansion Tube test conditions to evaluate the experimental results. These comparisons are detailed in Section 4.3. To contrast the three-dimensional (3D) analysis outcomes with the two-dimensional (2D) ones, shock patterns are studied at the geometry's symmetry plane which is illustrated in Figure 4.6. The numerical Schlieren image and Mach contour are provided in Figure 4.7 and Figure 4.8, respectively. The observed inlet shock

patterns and shoulder separation behavior exhibit similarities with the 2D case displayed in Figure 4.4.

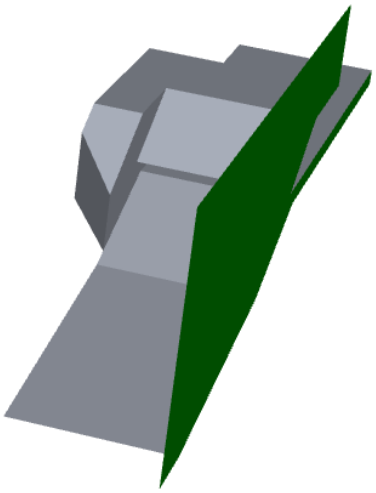

Figure 4.6. Symmetry Plane Illustration

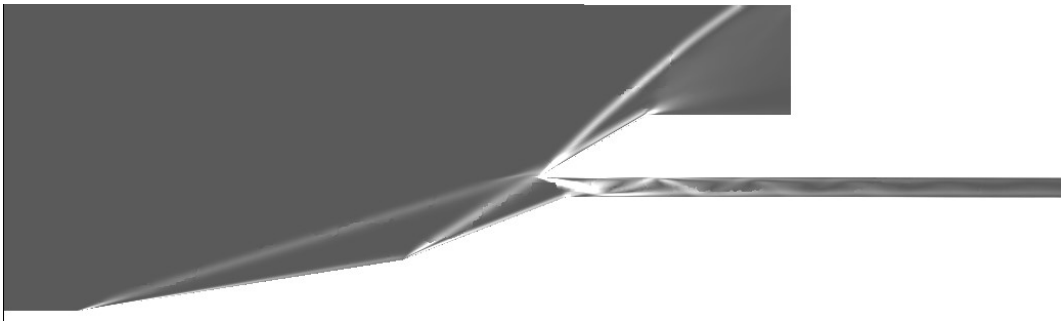

Figure 4.7. Numerical Schlieren - 3D CFD - Symmetry Plane

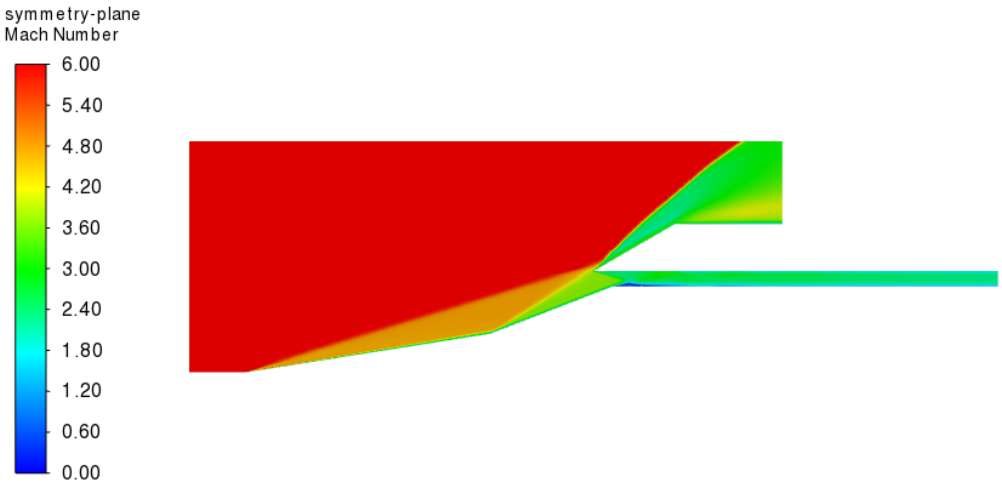

Figure 4.8. Mach Contour - 3D CFD - Symmetry Plane

Given the assumption of an ideal gas flow with constant specific heat, the Mach numbers following each shock can be compared to the 2D flight condition scenario. The relative difference with the 2D case is presented in Table 4.6. The 2D analysis demonstrates a strong agreement with the 3D analysis in terms of Mach number. Station properties derived from the 3D analysis results are shown in Table 4.7.

Table 4.6. Relative Difference between 3D and 2D Case

Parameter	**Relative Difference** (%)
M1	3.90
M2	4.52
M3	6.48

Table 4.7. Station Properties - 3D Case

Parameter	Value	Parameter	Value
M1	4.8	M3	2.85
P1	1.3 bar	P3	12.8 bar
T1	350K	T3	870K
M2	3.7	Outlet Mach	2.3
P2	4.8 bar	Outlet P	13.5 bar
T2	530K	Outlet T	940K

To assess the side-wall effects on the scramjet inlet flow, the Mach contour is initially examined in the midplane of the isolator, parallel to the incoming flow as illustrated in Figure 4.10, as displayed in Figure 4.9. It indicates that the inlet flow is disrupted around the sidewall, but this effect diminishes rapidly as the distance from the wall increases.

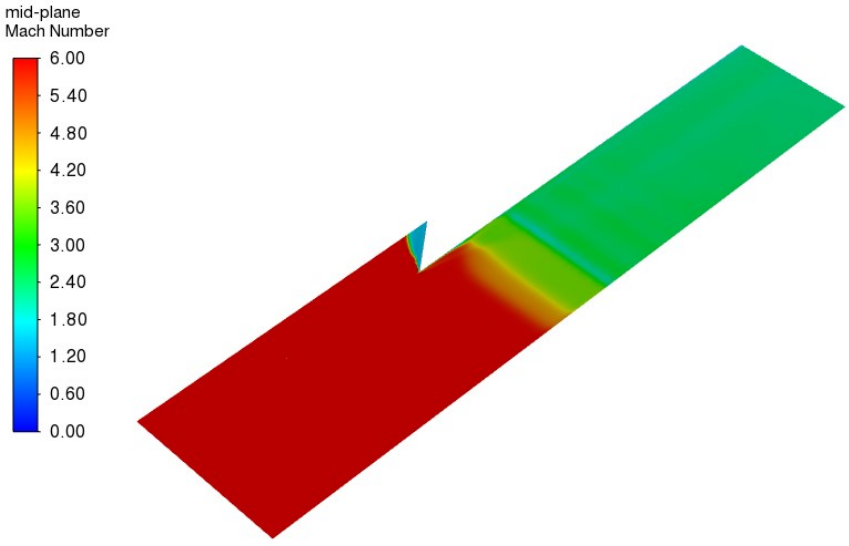

Figure 4.9. Mid-plane Mach Contour – 3D Case

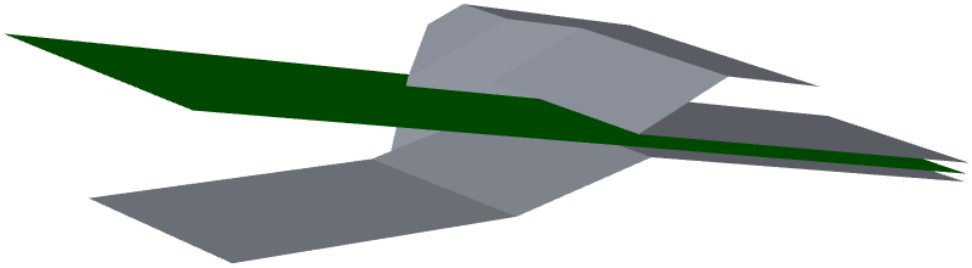

Figure 4.10. Isolator Mid-plane Illustration

For a more detailed examination of the sidewall effect, Mach contours in planes 4mm, 6mm, and 8mm away from the sidewall (parallel to the symmetry plane and side wall) are presented in Figure 4.11, Figure 4.12, and Figure 4.13, respectively. The sidewall effect is observed to decrease with increasing distance from the wall, and the flow structure resembles that of the symmetry plane when the distance reaches 8mm.

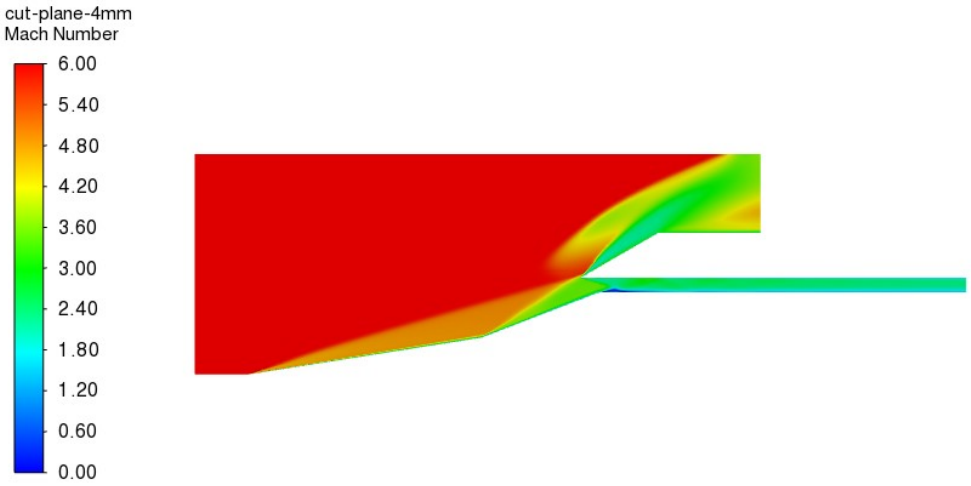

Figure 4.11. Mach Contour - 4mm Away from Sidewall - 3D Case

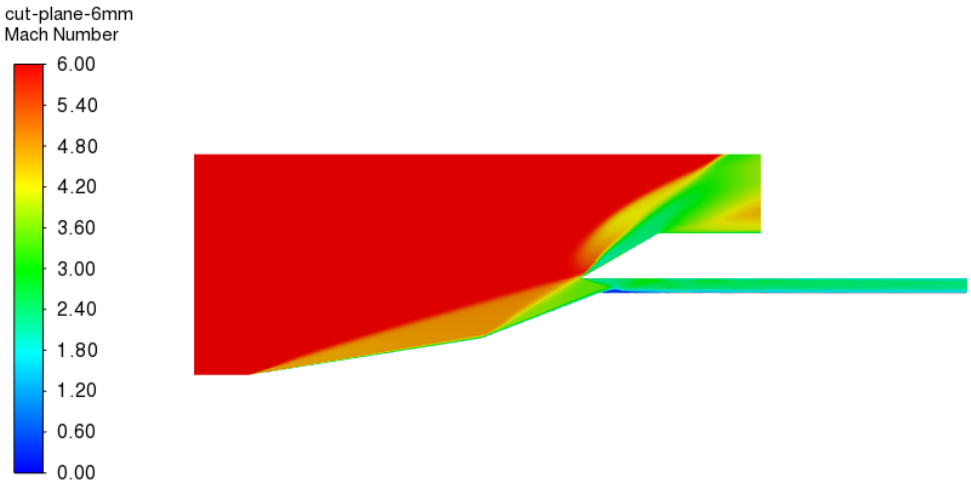

Figure 4.12. Mach Contour - 6mm Away from Sidewall - 3D Case

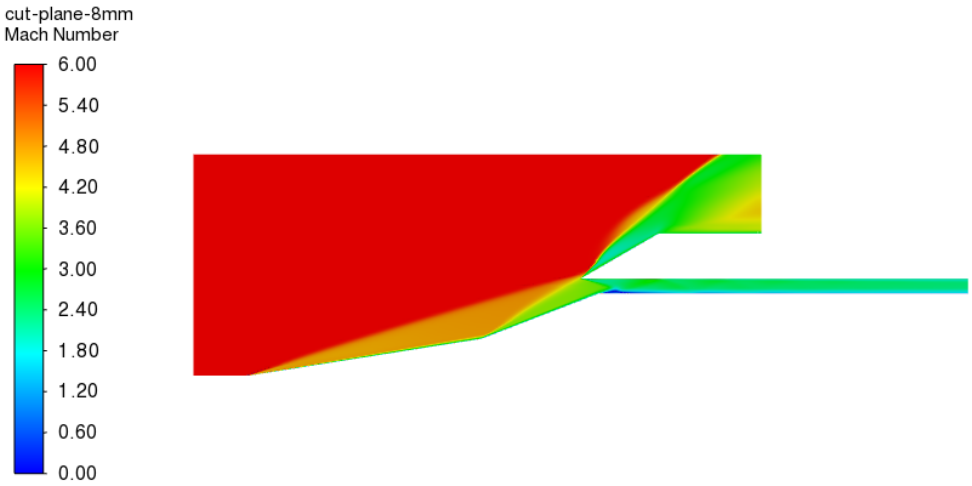

Figure 4.13. Mach Contour - 8mm Away from Sidewall - 3D Case

Lastly, the scramjet inlet's outlet conditions are investigated to observe the impact of both 3D effects and sidewall effects. Outlet Mach number contour, Mach number isolines, and static pressure contour are provided in Figure 4.14, Figure 4.15, and Figure 4.16. It is evident that although the Mach numbers at the outlet are nearly uniform, the compression ratio is lower around the sidewall.

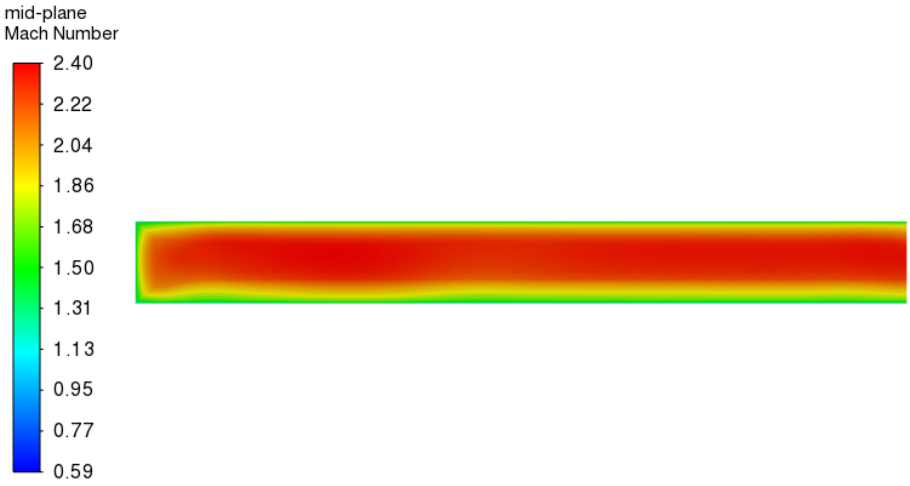

Figure 4.14. Outlet Mach Number Contour – 3D Case

Figure 4.15. Outlet Mach Isolines

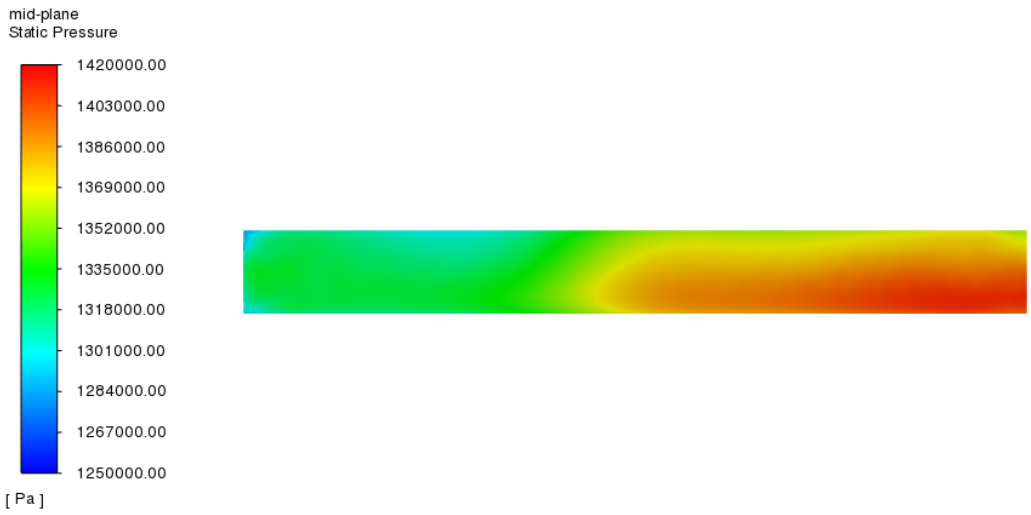

Figure 4.16. Outlet Static Pressure Contour – 3D Case

4.3 Investigation of Scramjet Inlet with Sudden Expansion Tube Experiments

The designed scramjet inlet is examined through a series of sudden expansion tube experiments, consisting of five tests conducted under three distinct test room conditions. Initially, three tests are performed at Mach 6, following the conditions outlined in Section 3.3. Measurements extracted from each test's Schlieren image are presented in Table 4.8, with Test 2's Schlieren image displayed in Figure 4.17. The relative difference between the 3D CFD analysis (from the symmetry plane) and the sudden expansion tube experiments is determined to be -0.82±1.4% for the Mach number after the first shock (M1) and 0.27±1.4% for the Mach number after the second shock (M2). These findings suggest that the experiments are in close alignment with the 3D CFD analysis results. Additionally, the shock patterns in the inlet, shoulder separation behavior, and shock-boundary layer interactions are found to be consistent with the 3D CFD outcomes. These flow behaviors are illustrated on the same Schlieren image as given in Figure 4.18.

Table 4.8. Results of Sudden Expansion Tube Experiments –Mach 6 Case

	Test1	**Test2**	**Test3**
First Shock Angle[°] (Wedge Angle 9°)	16.50±0.15	16.50±0.15	16.70±0.20
Upstream Mach Number[#]	6.10±0.10	6.1±0.10	5.96±0.13
Downstream Mach Number[#]	4.84±0.07	4.84±0.07	4.76±0.09
Expected Second Shock Angle[°] (Wedge Angle 21°)	30.65±0.15	30.65±0.15	30.83±0.20
Measured Second Shock Angle[°]	30.50±0.35	30.70±0.20	30.50±0.30
Upstream Mach Number[#]	4.90±0.15	4.82±0.08	4.90±0.13
Downstream Mach Number[#]	3.73±0.10	3.69±0.05	3.74±0.08

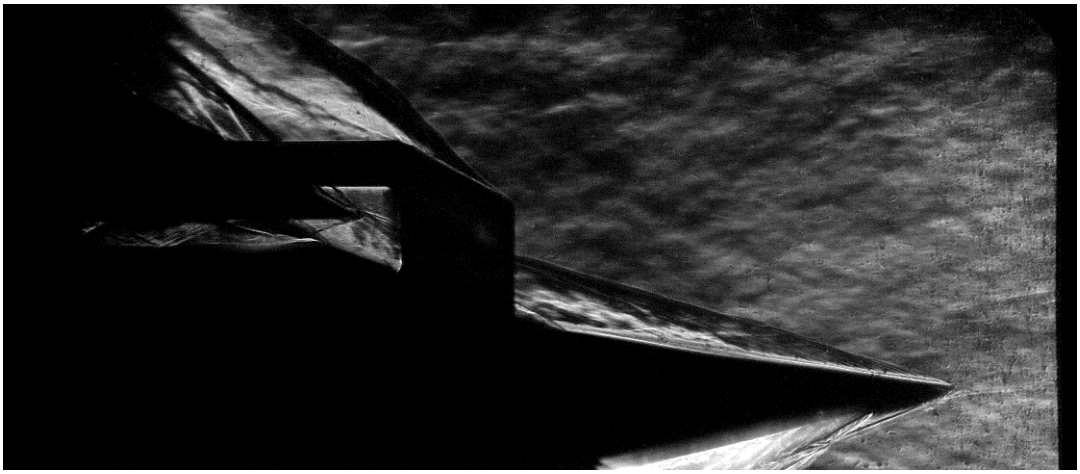

Figure 4.17. Schlieren Image – Scramjet Inlet Test2 – Mach 6 Case

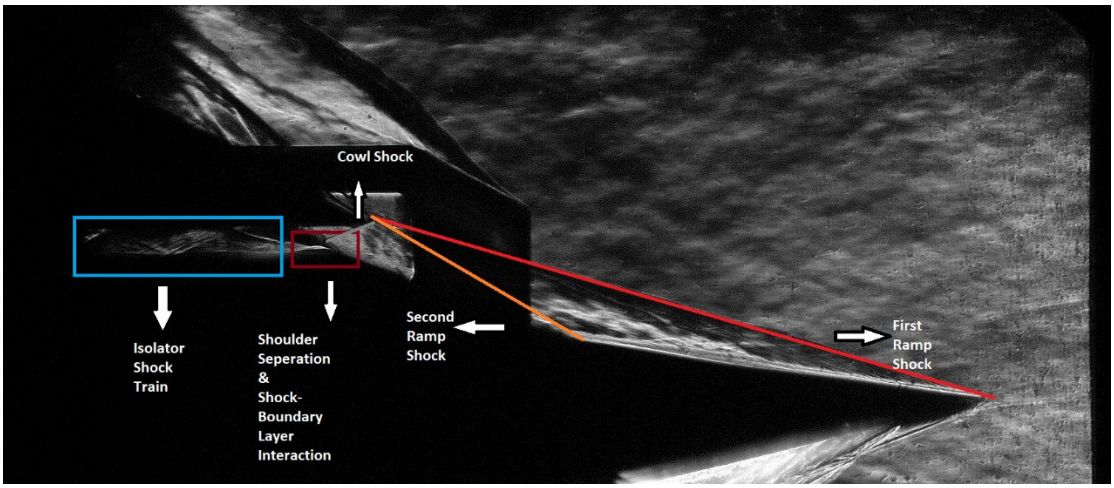

Figure 4.18. Schlieren Image - Scramjet Inlet Test2 - Mach 6 Case - with Explanations

Subsequently, off-design tests are conducted at Mach 5.5 and Mach 6.5. Measurements obtained from the Schlieren images are provided in Table 4.9, with the corresponding Schlieren images displayed in Figure 4.19 and Figure 4.20, respectively. Due to the poor quality of the Schlieren image for the Mach 6.5 case, the second shock angles could not be measured. In both instances, unstart behavior is not detected, and the flow remained supersonic within the isolator section of the inlet. Similar behaviors with Mach 6 (Figure 4.18) case are observed. These findings suggest that the designed inlet can be initiated within the Mach 5.5 to 6.5 range. However, additional analyses and experiments are required to further evaluate the inlet's performance at these specific Mach numbers.

Table 4.9. Results of Sudden Expansion Tube Experiments – Mach 5.5 and 6.5 Case

	5.5 Mach Case	**6.5 Mach Case**
First Shock Angle[°] (Wedge Angle 9°)	16.50±0.25	15.75±0.25
Upstream Mach Number[#]	5.48±0.10	6.68±0.19
Downstream Mach Number[#]	4.43±0.07	5.21±0.13
Expected Second Shock Angle[°] (Wedge Angle 21°)	31.70±0.20	29.85±0.25
Measured Second Shock Angle[°]	31.40±0.4	-
Upstream Mach Number[#]	4.54±0.20	-
Downstream Mach Number[#]	3.50±0.14	-

Figure 4.19. Schlieren Image – Scramjet Inlet Test – Mach 5.5 Case

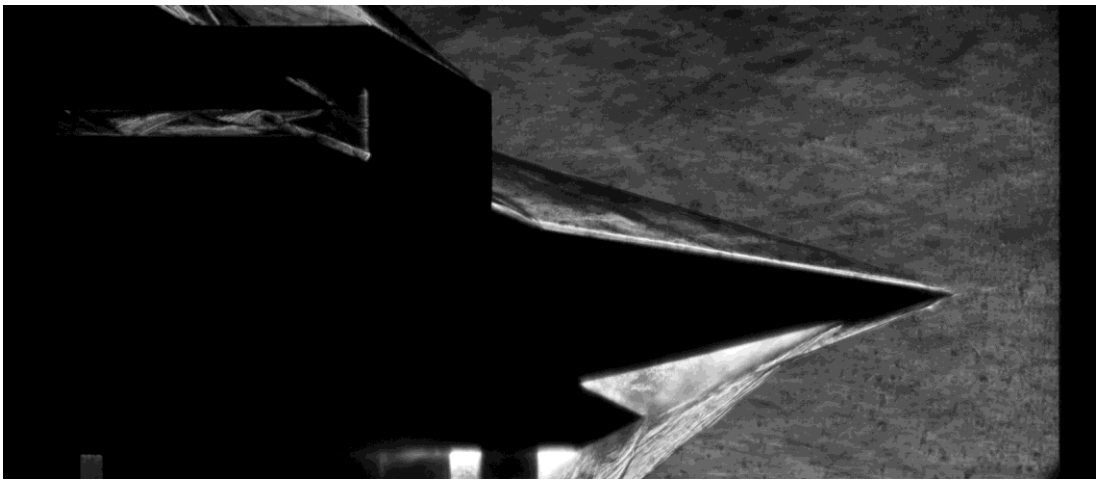

Figure 4.20. Schlieren Image – Scramjet Inlet Test – Mach 6.5 Case

CHAPTER 5

CONCLUSION

5.1 Conclusion Remarks

In this thesis, a 2D scramjet inlet that can operate at Mach 6 and 30km altitude is designed. First, 2D Inviscid CFD analysis is done to compare with design calculations, then viscous CFD analysis is done to observe viscous effects in inlet geometry. Second, 3D Viscous CFD analysis is done to observe both side-wall and 3D effects. Last, sudden expansion tube experiments are done to observe the performance of the inlet and compare it with 2D and 3D analyses.

Based on the results of the CFD simulations and sudden expansion tube experiments, it can be concluded that the 2D scramjet inlet designed in this study is feasible for operation at Mach 6 and 30 km altitude. The performance of the inlet is found to be in good agreement with the 1D estimations at the design point, and there are similar trends in pressure recovery and shock wave patterns observed in both the simulations and experiments, with minor differences in the details of the flow field. The effect of sidewalls is observed in the scramjet inlet's outlet conditions. Overall, the design process, which took into account considerations for flow stability, shock wave patterns, and pressure recovery, is successful in producing a viable inlet for operation under the specified conditions.

5.2 Future Work Recommendations

To improve the performance of the inlet in viscous conditions and determine and improve its operational envelope, additional CFD analyses and geometric optimization based on these analyses will be necessary. Testing will be required to validate the optimization method and relevant CFD analyses. Besides, sudden expansion tube experiments should be repeated with a suitable Schlieren imaging system for higher precision. To assess the performance of the inlet in off-design conditions, additional CFD analyses should be done.

REFERENCES

[1] Azam Che Idris, “Characterization of High Speed Inlets Using Global Measurement Techniques”, University of Manchester, 2014.

[2] S. Torrez, J. Driscoll, D. Dalle, and M. Fotia, “Preliminary Design Methodology for Hypersonic Engine Flowpaths,” in *16th AIAA/DLR/DGLR International Space Planes and Hypersonic Systems and Technologies Conference*, Oct. 2009. doi: 10.2514/6.2009-7289.

[3] M. Brown, N. Mudford, A. Neely, and T. Ray, “Robust Design Optimization of Two-Dimensional Scramjet Inlets,” in *14th AIAA/AHI Space Planes and Hypersonic Systems and Technologies Conference*, Nov. 2006. doi: 10.2514/6.2006-8140.

[4] S. O’Byrne, M. Doolan, S. R. Olsen, and A. F. P. Houwing, “Measurement and imaging of supersonic combustion in a model scramjet engine,” *Shock Waves*, vol. 9, no. 4, pp. 221–226, Aug. 1999, doi: 10.1007/s001930050159.

[5] M. K. Smart, “Optimization of Two-Dimensional Scramjet Inlets,” *J Aircr*, vol. 36, no. 2, pp. 430–433, Mar. 1999, doi: 10.2514/2.2448.

[6] W. H. Heiser and D. T. Pratt, *Hypersonic airbreathing propulsion*. American Institute of Aeronautics and Astronautics, 1994.

[7] Curran E.T and Murthy S.N.B, *Scramjet Propulsion*, vol. 189. AIAA, 2001.

[8] T. Nguyen, M. Behr, B. Reinartz, O. Hohn, and A. Gülhan, “Effects of Sidewall Compression and Relaminarization in a Scramjet Inlet,” *J Propuls Power*, vol. 29, no. 3, pp. 628–638, May 2013, doi: 10.2514/1.B34740.

[9] O. M. Hohn and A. Gülhan, “Experimental Characterization of Three-Dimensional Scramjet Inlet with Variable Internal Contraction,” *J Propuls Power*, vol. 38, no. 1, pp. 71–83, Jan. 2022, doi: 10.2514/1.B38315.

[10] NASA, “NASA Armstrong Fact Sheet: Hyper-X Program,” *NASA*, 2014.

[11] M. K. Smart, N. E. Hass, and A. Paull, “Flight Data Analysis of the HyShot 2 Scramjet Flight Experiment,” *AIAA Journal*, vol. 44, no. 10, pp. 2366–2375, Oct. 2006, doi: 10.2514/1.20661.

[12] T. J. Juliano, D. Adamczak, and R. L. Kimmel, “HIFiRE-5 Flight Test Results,” *J Spacecr Rockets*, vol. 52, no. 3, pp. 650–663, May 2015, doi: 10.2514/1.A33142.

[13] J. Hank, J. Murphy, and R. Mutzman, “The X-51A Scramjet Engine Flight Demonstration Program,” in *15th AIAA International Space Planes and Hypersonic Systems and Technologies Conference*, Apr. 2008. doi: 10.2514/6.2008-2540.

[14] K. Roberts and D. Wilson, “Analysis and Design of a Hypersonic Scramjet Engine with a Transition Mach Number of 4.00,” in *47th AIAA Aerospace Sciences Meeting including The New Horizons Forum and Aerospace Exposition*, Jan. 2009. doi: 10.2514/6.2009-1255.

[15] F. Bramkamp, Ph. Lamby, and S. Müller, “An adaptive multiscale finite volume solver for unsteady and steady state flow computations,” *J Comput Phys*, vol. 197, no. 2, pp. 460–490, Jul. 2004, doi: 10.1016/j.jcp.2003.12.005.

[16] Y. Wada and M.-S. Liou, “An Accurate and Robust Flux Splitting Scheme for Shock and Contact Discontinuities,” *SIAM Journal on Scientific Computing*, vol. 18, no. 3, pp. 633–657, May 1997, doi: 10.1137/S1064827595287626.

[17] W.-Y. Su, Z. Hu, P.-P. Tang, and Y. Chen, “Transient Analysis for Hypersonic Inlet Accelerative Restarting Process,” *J Spacecr Rockets*, vol. 54, no. 2, pp. 376–385, Mar. 2017, doi: 10.2514/1.A33601.

[18] D. C. Wilcox, “Dilatation-dissipation corrections for advanced turbulence models,” *AIAA Journal*, vol. 30, no. 11, pp. 2639–2646, Nov. 1992, doi: 10.2514/3.11279.

[19] O. M. Hohn and A. Gülhan, “Experimental Characterization of Three-Dimensional Scramjet Inlet with Variable Internal Contraction,” *J Propuls Power*, vol. 38, no. 1, pp. 71–83, Jan. 2022, doi: 10.2514/1.B38315.

[20] J. Häberle and A. Gülhan, “Investigation of Two-Dimensional Scramjet Inlet Flowfield at Mach 7,” *J Propuls Power*, vol. 24, no. 3, pp. 446–459, May 2008, doi: 10.2514/1.33545.

[21] Kyle Charles Markell, “Exergy Methods for the Generic Analysis and Optimization of Hypersonic Vehicle Concepts ,” 2005.

[22] J. McGuire, R. Boyce, and N. Mudford, “Comparison of Computational and Experimental Studies on Shock Induced Ignition in Scramjets,” in *AIAA/CIRA 13th International Space Planes and Hypersonics Systems and Technologies Conference*, May 2005. doi: 10.2514/6.2005-3394.